Results in Engineering 24 (2024) 102932

Contents lists available at ScienceDirect

Results in Engineering

journal homepage: www.sciencedirect.com/journal/results-in-engineering

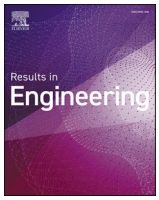

Computational fluid dynamic simulation of earth air heat exchanger: A thermal performance comparison between series and parallel arrangements

Sarwo Edhy Sofyan [a,*], Teuku Meurah Indra Riayatsyah [b,c,**], Khairil [a], Eric Hu [d], Akram Tamlicha [a], Teuku Muhammad Reza Pahlefi [a], H.B. Aditiya [e,f,g]

[a] Department of Mechanical Engineering, Universitas Syiah Kuala, Banda Aceh, 23111, Indonesia
[b] Program Study of Mechanical Engineering, Department of Production and Industrial Technology, Institut Teknologi Sumatera, 3536, South Lampung, Indonesia
[c] Centre for Technology in Water and Wastewater, School of Civil and Environmental Engineering, Faculty of Engineering and Information Technology, University of Technology Sydney, NSW, 2007, Australia
[d] School of Electrical and Mechanical Engineering, University of Adelaide, Adelaide, SA, 5005, Australia
[e] Department of Mechanical Engineering, Faculty of Engineering and Technology, Sampoerna University, Jakarta, Indonesia
[f] Sampoerna University Energy Research Center, Pancoran, Jakarta Selatan 12780, Indonesia
[g] Faculty of Engineering and IT, University of Technology Sydney, 81 Broadway, Ultimo, NSW, 2007, Australia

ARTICLE INFO

Keywords:
EAHE arrangements
CFD simulation
Thermal performance
Effectiveness-NTU
Passive Cooling

ABSTRACT

This study uses Ansys Fluent to compare the thermal performance of series and parallel earth air heat exchanger (EAHE) systems for cooling. The model was validated using experimental data from published literature and matched simulation results. The sensitivity study examined how length, diameter, and ground surface coverings affected EAHE performance. The relationship between effectiveness and the Number Transfer Unit (NTU) of EAHE was explored along with the soil thermal regime. The simulation results show that the series EAHE can achieve a lower temperature drop than parallel. With an input air temperature of 32 °C and EAHE lengths varying from 10 m to 50 m (in 10 m increments), the 50 m EAHE produced the lowest outlet air temperatures: 27.2 °C for the series configuration and 28.8 °C for the parallel arrangement. Changing the EAHE diameter (4–6 in) results in a ±0.2 °C outlet air temperature drop for both setups. EAHE performed best under short grass soil cover, yielding 1.4 °C and 0.5 °C lower outlet air temperatures, for series and parallel arrangements than the asphalt cover. The pressure drop increased proportionally with EAHE's length. Simulation results indicate a ±6 times larger pressure loss in the series design compared to the parallel setup. The effectiveness-NTU relationship shows that parallel EAHEs are 15 % more effective than series ones.

1. Introduction

Buildings use a significant amount of energy, accounting for around 40 % of global energy consumption. The majority of the energy used in buildings is for heating, ventilation, and air conditioning (HVAC) [1]. Heat pumps/air conditioning systems that operate on a vapor compression cycle are now used to offer indoor thermal comfort for inhabitants. These heating/cooling systems use a lot of energy (primarily for the compressor), which adds to the operating costs. Other low-energy cooling/heating methods, such as Maisotsenko cycle indirect evaporative cooling [2] and earth air heat exchanger (EAHE) cooling/heating systems have been introduced [3–7].

EAHE is a basic heating/cooling technique that uses a relatively consistent ground temperature rather than the surrounding air to provide heating (in winter) and cooling (in summer). EAHE is a reasonably simple system that circulates ambient air via a buried PVC pipe to exchange heat with the surrounding soil to produce indoor heating or cooling. To offer indoor cooling, ambient air that is warmer than the ground temperature is pumped through the PVC pipe, releasing heat to the surrounding earth. The temperature of the circulated air reduces several degrees Celsius as a result of the heat transfer process [8].

The effectiveness of EAHE systems has been assessed under a variety of circumstances using parametric analysis [9–12]. The impact of a few design parameters (pipe diameter, input condition, pipe length, and

* Corresponding author.
** Corresponding author.
E-mail addresses: sarwo.edhy@usk.ac.id (S.E. Sofyan), indraayat@gmail.com (T.M.I. Riayatsyah).

https://doi.org/10.1016/j.rineng.2024.102932
Received 17 June 2024; Received in revised form 2 September 2024; Accepted 17 September 2024
Available online 19 September 2024

outlet condition) on the overall functionality of the EAHE system has been examined numerically in a study presented by Hasan et al. [13]. To assess the effectiveness of the chosen cooling system, the following metrics are utilised: return period, overall power savings, power conservation, and cost reduction. Also, the impact of a few design parameters (pipe diameter, input condition, pipe length, and outlet condition) on the overall functionality of the EAHE system has been examined numerically [14]. A new modelling tool, an examination of parametric influence, and an optimising criterion were all created by Li et al. [15]. In this work, a 1D-2D hybrid transient numerical model was constructed by incorporating into the earth domain a pair of 1D implicit convection-diffusion models and several 2D explicit diffusion models. The output temperature, humidity, and yearly cooling/heating capacity of the EAHE were considered when analysing its thermal performance.

The study of multi-pipe EAHE has been studied by several researchers [16–20]. Qi et al. [20] presented an empirical model of multi-pipe parallel EAHE that was validated using experimental data. The airflow uniformity coefficient and integrated evaluation factor were introduced to assess the uniformity and thermal performance of EAHE. In addition, a comparison was made regarding the impact of structural characteristics on the thermal efficiency of EAHE. These parameters encompassed the distance between pipes, the depth of pipes, and the angle of the branch pipe at which the airflow enters. The findings indicated that the heat exchange rate was maximized and the air dispersion was more evenly distributed when the spacing between pipes and the depth of pipes were set at 1.2 m and 3 m, respectively.

The taguchi method has been applied in the optimisation of EAHE [21–23]. Qi et al. [21] optimised the multi-pipe EAHE for usage in greenhouses and other environments with high relative humidity using the Taguchi approach. After building a full-scale model of a greenhouse, they tested it out using real-time monitoring data to confirm its temperature conditions. To assess their combined efficacy, EAHE parameters underwent multivariate analysis. The greenhouse was subsequently equipped with the most effective mix of designs. According to the results, the inlet air temperature had the greatest impact on the EAHE system's integrated performance, accounting for 45.2 % of the total. The input air velocity came next at 22 % while the pipe diameter came in at 18.4 %.

The current literature [1–23] has examined the latest developments in EAHE research. Nevertheless, there has not been a thorough investigation comparing the thermal performance of series and parallel EAHE systems in the tropical climate of Banda Aceh, Indonesia. This study aims to investigate the thermal performance comparison between series and parallel EAHE configurations using computational fluid dynamics (CFD) simulation in the tropical climate of Banda Aceh, Indonesia. The study considers the impact of EAHE pipe length, diameter, and ground surface cover. Furthermore, the study also examines the soil's thermal behaviour near the EAHE and the correlation between EAHE effectiveness and the Number of Transfer Units (NTU).

2. Soil thermal characteristics and simulation method

2.1. Soil temperature and thermo-physical properties

Soil temperature on the earth's surface is influenced by a number of factors, such as solar radiation, air temperature, rainfall, soil type, soil surface, etc. Soil temperature fluctuations decrease rapidly with increasing depth and become negligible at 3–5 m depth. At this depth, the soil temperature remains nearly constant all year round. This undisturbed soil temperature is lower than the ambient air temperature in summer and higher during winter [24–26]. This low-enthalpy geothermal energy can be harnessed for space cooling and heating applications using EAHE. When installing the EAHE, it is necessary to determine the subsurface temperature. Kusuda and Achenbach [27] provide an empirical relationship to calculate the subsoil temperature at each location, time, and depth as:

$$T_{soil\ (Z,t)} = T_{mean} - T_{amp}\ x\ exp\left(- z\sqrt{\frac{\pi}{365\ x\ \alpha}\ x\ cos\left[\frac{2\pi}{365\ x\ \alpha}\left(t_{year} x\ t_{shift} - \frac{z}{2}\sqrt{\frac{365}{\pi\ x\ \alpha}}\right)\right]}\right) \quad (1)$$

Similarly, Derbel and Kanoun [28] developed a correlation to calculate the underground temperature as:

$$T_{soil\ (Z,t)} = T_{mean} + A.\cos\left[\omega\left(t_{year} - t_{shift}\right) - \frac{Z}{d}\right] e^{-\frac{z}{d}} \quad (2)$$

Several studies have shown that daily and annual variations in soil temperature do not penetrate deeper than 0.5 m and 4.0 m, respectively. Popiel et al. [29] compared variations in soil temperature with depth on bare and grass-covered surfaces. It was observed that during summer, the underground temperature at 1 m depth was 4 °C higher on the bare surface compared to the grass-covered surface [30]. In addition, Sanusi et al. [31] found maximum soil temperatures of 28.6 °C, 28.5 °C, and 28.3 °C in the rainy season and 30.1 °C, 30.2 °C, and 30.3 °C in the summer in depths of 1.5 m, 1.0 m, and 0.5 m, respectively, under the hot and humid climate of the Malaysian area. It is also reported that the pipes at a depth of 1 m from the ground surface are the most economical for EAHE systems. Wu et al. [32] evaluated the thermal performance of an EAHE system considering pipes at 1.6 m and 3.2 m depth for summer cooling operations. The examination revealed that the air temperature was lower at a depth of 3.2 m (ranging from 25.7 °C to 30.7 °C) than at a depth of 1.6 m (ranging from 27.2 °C to 31.7 °C). Generally, the cooling/heating potential of EAHE systems increases with installation depth. After reaching a certain depth, EAHE systems do not show a substantial performance improvement. In addition, the trenching costs increase with pipe depth. The rate of heat transfer and the distribution pattern of temperatures in the soil domain adjacent to EAHE are directly impacted by the thermophysical characteristics of the soil. Lekhal et al. [33] summarises several thermal properties of soil as shown in Table 1.

2.2. Albedo

Albedo is a quantity that describes the ratio between sunlight arriving at the surface of the earth and being reflected into space with a change in wavelength (outgoing longwave radiation). The difference in wavelength between the incoming and the reflected can be related to how much solar energy is absorbed by the earth's surface. A solid surface gives a greater albedo value than a soft surface. In general, urban areas have a greater albedo value than agricultural or forestry areas, so "hot islands" are always a serious case in urban areas. Yilrnaz et al. [34] studied the temperature differences between concrete surfaces, asphalt, ground surfaces, and grassy surfaces in Erzurum City in Turkey, and they reported an average temperature difference of 6.5 °C between asphalt and soil, 5.3 °C between soil and grass, and 11.8 °C between asphalt and grass surfaces. The same modelling procedure as above was applied by Fuji et al. [35] to calculate the heat transfer in soil and pipes. As the initial condition of the numerical model, the soil temperature measured at the test site was entered for each layer. All peripheral and lower limits were defined as constant temperatures concerning the measured values. In addition, the energy balance was considered at the soil surface using **Equation (3)** and the temperature distribution was calculated in the

Table 1
The thermophysical properties of the typical soil [33].

Type of soil	Conductivity W/(mK)	density kg/m^3	Heat Capacity J/(kgK)
Muddy clay	1.5	1530	920
sandy	0.9	1780	1390
Muddy sand	2.6	970	1518

shallow soil.

$$Q = R_{sol} + R_{sky} - R_{surf} - H_{surf} - L_{surf} \quad (3)$$

The calculation of the energy balance at the ground surface can be simplified using soil-air temperature (SAT) as shown in Equation (4).

$$SAT = \theta_0 + \frac{1}{\alpha_0((1-\alpha_S)J - \varepsilon J_{eh}} \quad (4)$$

The albedo value, α_0, for bare soil is equal to 0.3. The longwave emissivity, denoted as ε, is 0.9, which is a typical value for soil. The overall heat transfer coefficient, α_0, is the combination of the convective heat transfer coefficient, α_c, and the radiative heat transfer coefficient, α_r. The value of α_r is given that corresponds to 5.1 W/(m^{2}K). The value of α_c is determined using the Jürges equation based on the wind speed, v (m/s), as:

$$\alpha_c = 5.8 + 3.9\, v \; (v < 5\, m/s) \quad (5)$$

$$\alpha_c = 7.1\, v^{0.78} \; (v > 5\, m/s) \quad (6)$$

Effective emission, $J_{eh,}$ is calculated using Equation (7) as:

$$J_{eh} = \sigma \; (273.16 + \theta_0)^4 \left(0.474 + 0.076 f^{1/2}\right) \quad (7)$$

where σ and f are the Stefan-Boltzmann constant ($= 5.67\, x\, 10^{-8} \frac{w}{m^2}/K$) and the water vapor pressure (mmHg) above the soil surface, respectively.

2.3. The Effectiveness-NTU of EAHE

Bergman et al. [36] reported that effectiveness is the ratio of the actual heat transfer rate of the heat exchanger to the maximum possible heat transfer rate. The effectiveness equation is expressed as:

$$\varepsilon = \frac{q}{q_{max}} \quad (8)$$

NTU stands for Number of Transfer Units, which is a dimensionless parameter used widely in heat exchanger analysis. NTU is defined as the number of transfer units. Incropera also provides an equation regarding NTU:

$$NTU = \frac{UA}{C_{min}} \quad (9)$$

where U is the overall heat transfer coefficient. U is defined as the total resistance experienced as heat that is transferred between substances, and A is the surface area (m). The relationship between effectiveness and NTU can be seen in Equation (10) by Yusof et al. [1]:

$$\varepsilon = 1 - e^{-NTU} \quad (10)$$

where ε is the effectiveness of the heat exchanger. Equation (10) can be rearranged and presented as:

$$\varepsilon = 1 - e^{UA_s \; / \; m_{air} cp} \quad (11)$$

2.4. Governing equations for computational fluid dynamics

The fundamental equations for fluid flow and heat transfer are generally governed by the three conservation laws, namely the equations of continuity, conservation of momentum, and conservation of energy, which are shown as follows [37]:

Continuity equation:

$$\frac{\partial u}{\partial x} + \frac{\partial v}{\partial y} + \frac{\partial w}{\partial z} = 0 \quad (12)$$

The x-momentum equation:

$$\left[u\frac{\partial u}{\partial x} + v\frac{\partial u}{\partial y} + w\frac{\partial u}{\partial z}\right] = -\frac{1}{\rho}\frac{\partial P}{\partial x} + \vartheta\left[\frac{\partial^2 u}{\partial x^2} + \frac{\partial^2 u}{\partial y^2} + \frac{\partial^2 u}{\partial z^2}\right] \quad (13)$$

The y-momentum equation:

$$\left[u\frac{\partial v}{\partial x} + v\frac{\partial v}{\partial y} + w\frac{\partial v}{\partial z}\right] = -\frac{1}{\rho}\frac{\partial P}{\partial y} + \vartheta\left[\frac{\partial^2 v}{\partial x^2} + \frac{\partial^2 v}{\partial y^2} + \frac{\partial^2 v}{\partial z^2}\right] \quad (14)$$

The z-momentum equation:

$$\left[u\frac{\partial w}{\partial x} + v\frac{\partial w}{\partial y} + w\frac{\partial w}{\partial z}\right] = -\frac{1}{\rho}\frac{\partial P}{\partial z} + \vartheta\left[\frac{\partial^2 w}{\partial x^2} + \frac{\partial^2 w}{\partial y^2} + \frac{\partial^2 w}{\partial z^2}\right] \quad (15)$$

Energy conservation equation:

$$\left[u\frac{\partial T}{\partial x} + v\frac{\partial T}{\partial y} + w\frac{\partial T}{\partial z}\right] = \alpha\left[\frac{\partial^2 T}{\partial x^2} + \frac{\partial^2 T}{\partial y^2} + \frac{\partial^2 T}{\partial z^2}\right] \quad (16)$$

From Equations 12–16, u, v, and w are the velocities of the components in the x, y, and z directions. P and T are the pressure and temperature respectively, ϑ is the kinematic viscosity, and α is the thermal diffusivity.

2.5. Geometry of EAHE

The EAHE pipes' geometry was generated using Autodesk Inventor software and subsequently exported to the design modeler in ANSYS software. In this study, the geometry of EAHE consists of a sequence in series and parallel where the working fluid (air) circulates and the soil serves as a heat sink. The EAHE pipe is made of polyvinyl chloride (PVC) and its dimensions (in mm units) are presented in Fig. 1. The figure illustrates that the EAHE has a burial depth of 2000 mm and a span between the pipes of 1000 mm. The computational domain of EAHE is illustrated in Fig. 2. The Boolean tool was used to combine the pipe and soil domains to obtain the results of a pipe embedded in the ground, as shown in Fig. 2.

2.6. Meshing and material properties

The tetrahedron mesh was used to discretise both EAHE and the soil domain, as illustrated in Fig. 3. Following the completion of meshing, the next step involves the identification of geometric areas that include inlet, outlet, air domain, soil, and surface as shown in Fig. 4. Table 2 shows the material properties used in the simulation.

2.7. Initial and boundary conditions

The initial condition of the soil and EAHE was set to 25 °C. In addition, different boundary conditions were applied to the computational domain of EAHE. The inlet air temperature and the boundary condition for the soil domain were set based on the climate and geological conditions in Banda Aceh, Indonesia. The constant soil temperature (25 °C) was applied on the lateral and bottom sides of the soil domain. The soil surface was assumed to be bare soil, and its temperature was determined by using Equation (4), which corresponds to 32.1 °C. The temperature and mass flow rate of the air, namely 32 °C and 0.04 kg/s, respectively, were set for the inlet boundary of EAHE. While an outflow boundary condition was applied for the outlet of EAHE. The heat transfer was coupled at the EAHE pipe-soil interface. In addition, no-slip conditions for velocity were applied at the EAHE pipe surface, and the standard K-epsilon model was applied in the simulation. The boundary conditions used for the EAHE simulation are summarised in Table 3.

To ensure computational feasibility, several key assumptions were made.

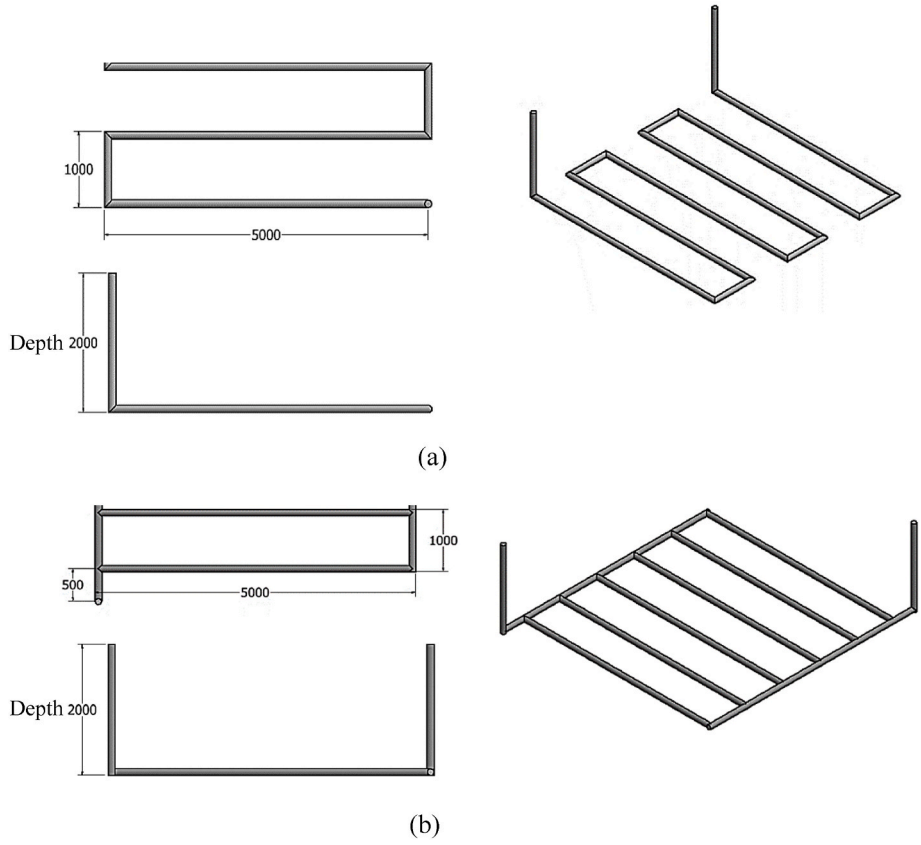

Fig. 1. Geometry of EAHE: (a) series arrangement; (b) parallel arrangement.

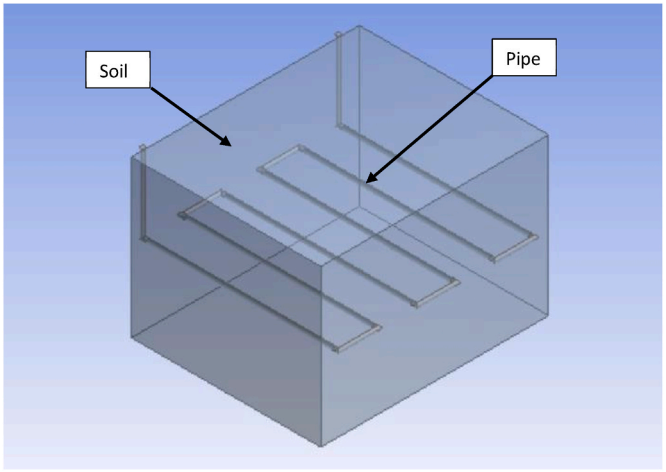

Fig. 2. Computational domain of EAHE.

i. The air's physical properties, such as density and specific heat capacity, were considered constant during the simulation because the system experienced a narrow temperature range.
ii. The air temperature and velocity at the inlet were assumed to be constant and uniform.
iii. The surrounding soil was represented as a homogenous, isotropic material.
iv. The soil maintains constant physical properties and temperature.
v. A three-dimensional model of EAHE is assumed to be in steady state.
vi. The soil is rigid and completely in contact with the EAHE pipe.
vii. No slip boundary condition at the pipe's wall of EAHE.

3. Mesh sensitivity analysis

The number of mesh elements depends on the element size. As the size of the element increases, the number of elements decreases, and vice versa. The size of the elements must be reduced for good-quality computational fluid dynamic results. At certain element sizes, the resulting quality will improve due to size reduction. Table 4 shows the value of the meshing size and the number of grid elements to the estimated outlet air temperature of EAHE. Fig. 5 illustrates the profile of EAHE's outlet air temperature under various mesh's number of elements. The findings demonstrate that there is no significant difference in EAHE's outlet air temperature due to variations in the number of elements. Thus, it can be concluded that the mesh size has acceptable quality. At the number of elements of 980385, it was found that the outlet air temperature of the EAHE is 29.6 °C.

4. Model validation

In this study, model validation is limited to the series EAHE arrangement. This is regarded as sufficient because both series and parallel types of EAHE have identical boundary conditions, thermal characteristics, and assumptions, except for their arrangement. The simulation results were validated using experimental data conducted by Manik et al. [38]. Table 5 shows the specifications of the EAHE used for validation. The material properties for validation of EAHE are illustrated in Table 6.

Table 7 compares the simulation and Manik et al.'s work at three different recording times, namely 12:00 a.m., 1:00 p.m., and 2:00 p.m. The average error in outlet air temperature was found to be 0.93 %. It is clear from the table that the comparison of the experimental and simulated outlet air temperature (T_{out}) results shows satisfactory findings. Thus, it can be said that the simulation model used in this study is

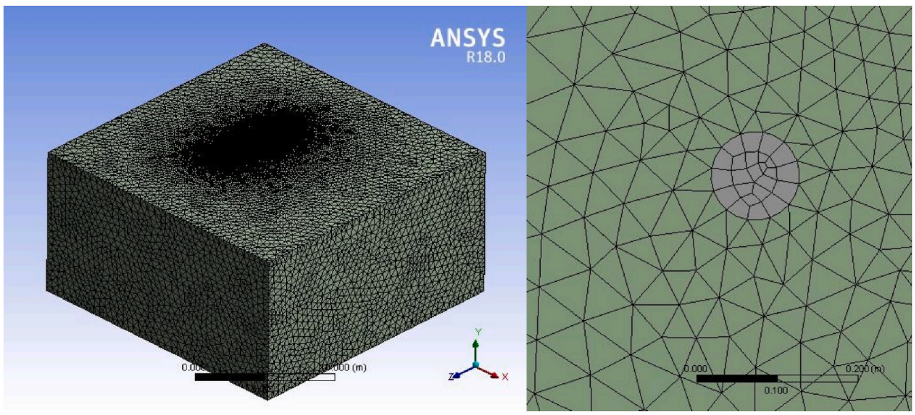

Fig. 3. The mesh of EAHE.

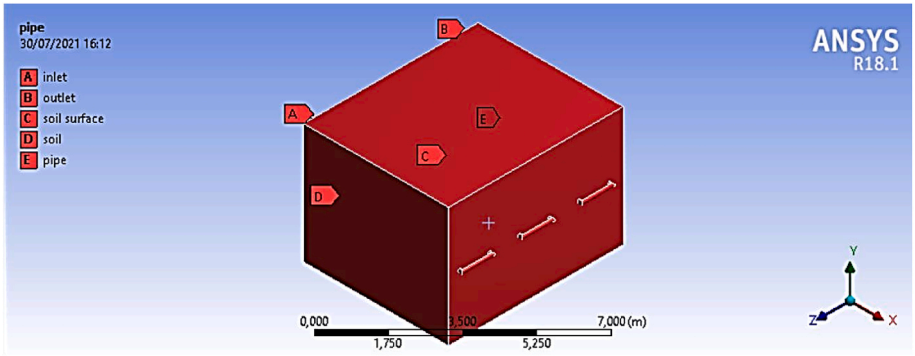

Fig. 4. EAHE name selection.

Table 2
Material properties of EAHE.

Material	Density kg/ m^3	Specific Heat J/ (kgK)	Thermal Conductivity W/ (mK)
Soil	2000	1489	1
PVC	1400	1005	0.19
Air	1.225	1006.43	0.0242

Table 3
The boundary conditions.

Boundary Conditions	Setup	Value
Inlet	Mass flow rate	0.04 kg/s
	Temperature	32 °C
Outlet	Outflow	–
EAHE's inner pipe surface	No slip	–
Upper surface of soil	Temperature	32.1 °C (for bare soil)
Lower surface of soil	Temperature	25 °C
Lateral surface of soil	Temperature	25 °C

Table 4
Mesh sensitivity on outlet air temperature of EAHE.

Element size on the ground (m)	Element size on the pipe (m)	Number of Elements	T_{out} (°C)
0.1	0.001	3103337	29.633
0.15	0.002	1008843	29.655
0.2	0.003	980385	29.655
0.25	0.004	963706	29.658
0.3	0.005	962324	29.652

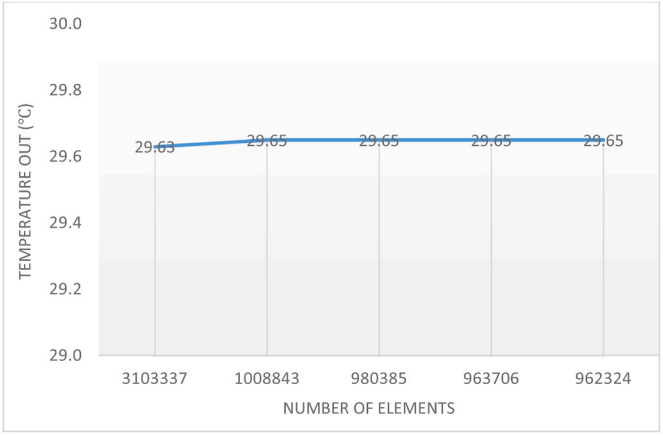

Fig. 5. Effect of the number of elements on the EAHE's outlet air temperature.

Table 5
EAHE specifications for validation.

Technical parameters	Remarks
Pipe diameter	0.1016 m
Pipe length	26.5 m
Soil depth	2 m
Working fluid	Air
Inlet air velocity	3 m/s
Initial soil temperature	27 °C

Table 6
Material properties for validation of EAHE.

Material	Density kg/m^3	Specific Heat J/(kgK)	Thermal Conductivity W/(mK)
Clay soil	1300	1004	1.3
PVC	1400	1005	0.19
Air	1.225	1006.43	0.0242

Table 7
Comparison between experimental data and simulation results.

T_{in}	T_{soil}	T_{out} Experiment	T_{out} Simulation	Error
30 °C	26.9 °C	28.7 °C	29.03 °C	1.14 %
31.2 °C	26.7 °C	29.3 °C	29.65 °C	1.18 %
31.4 °C	26.9 °C	29.7 °C	29.84 °C	0.47 %

reliable.

5. Results and discussion

This section presents the sensitivity analysis of both EAHE arrangements, considering the effects of EAHE's pipe length, diameter, and types of ground surface covers. The association between NTU and the effectiveness, pressure drop, and soil temperature contours surrounding EAHE were also investigated.

5.1. The effect of EAHE's length on the outlet air temperature

The length of an EAHE can significantly influence the outlet air temperature in HVAC systems. Fig. 6 illustrates the comparison of outlet air temperature produced by series and parallel arrangements of EAHE under five different lengths of EAHE, namely 10–50 m with an increment of 10 m. From the figure, it can be seen that the series arrangement of EAHE yields a relatively lower outlet air temperature compared to that of the parallel arrangement. This result shows that the series arrangement generates higher air temperature differences between the inlet and the outlet. This phenomenon is influenced by the relatively longer path for air to flow, resulting in a lower air temperature at the outlet of EAHE. The temperature difference between the incoming air and the ground can influence the outlet air temperature, which may vary across the heat exchanger's length. The ideal length of an EAHE can differ based on the climate of a location [39–42]. In colder climates, a longer heat exchanger might be necessary to extract an adequate amount of heat from the ground, whereas, in warmer climates, a shorter heat exchanger could be more efficient. As can be observed from Fig. 6, it is evident that the EAHE with a 10 m total pipe length produces the least decrease in outlet air temperature. The outlet temperature for the series pipe is 29.6 °C, while for the parallel pipe, it is 30.3 °C. The EAHE, which has a total length of 50 m, is capable of achieving lower outlet air temperatures of up to 27.2 °C for the series arrangement and 28.8 °C for the parallel arrangement. Furthermore, on the 10 m long pipe, the outlet air temperature is decreased by 2.3 °C from the inlet air temperature for the series pipe and 1.7 °C for the parallel pipe. Meanwhile, at a pipe length of 50 m, the outlet air temperature is 4.7 °C lower than the inlet temperature in the series pipe and 3.2 °C lower in the parallel pipe. The effectiveness of heat transfer between air and ground greatly depends on the length of the heat exchanger. The increased length of an earth-air heat exchanger provides a greater area for exchanging heat with the surrounding soil, which improves its ability to transfer heat. This increased surface area enables more efficient cooling or heating of the incoming air.

5.2. The effect of EAHE diameter on outlet air temperature

Fig. 7 illustrates the relationship between the diameter of EAHE over the outlet air for both series and parallel arrangements. The size of EAHE's diameter is an essential factor that profoundly impacts the final air temperature in geothermal heating and cooling systems. As can be observed from the figure, the decrease in outlet air temperature is directly proportional to the increase in the diameter of EAHE. The pipe diameter affects the rate of heat exchange which ultimately determines the temperature of the air leaving the EAHE. A greater pipe diameter of EAHE facilitates heat transfer enhancement with the surrounding earth. This expanded surface area improves the thermal contact, thereby facilitating the heat exchange between the circulated air and the ground. Consequently, in cooling applications, the outlet air temperature tends to be lower as the system can efficiently release thermal energy. On the contrary, a decrease in diameter could restrict the heat exchange capability, resulting in less efficient temperature regulation. The diminished surface area within narrower pipes might impede the system's efficiency in transferring heat, thereby affecting both its overall performance and the desired temperature of the air being released [43, 44]. It was found that the thermal performance of the parallel EAHE is inferior compared with the series arrangement. This tendency is shown through the comparison of the outlet air temperature produced, where the parallel arrangement produces a temperature corresponding to 1 °C higher than that produced by the series arrangement. The 4 in diameter of EAHE produces a temperature difference between the inlet and outlet of 3.9 °C and 2.9 °C for series and parallel configurations, respectively. When the EAHE pipe diameter is increased to 6 in, the temperature difference increases to 4.1 °C and 3.1 °C, respectively. Furthermore, it was found that increasing the EAHE pipe diameter from 4 in to 6 in only resulted in a temperature reduction of 0.2 °C for both setups.

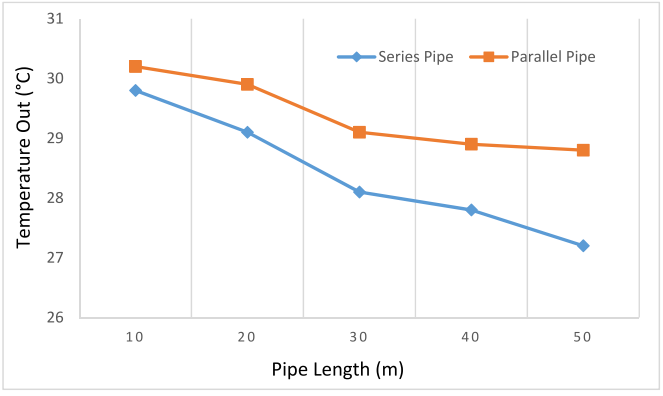

Fig. 6. Effect of EAHE's length on the outlet air temperature.

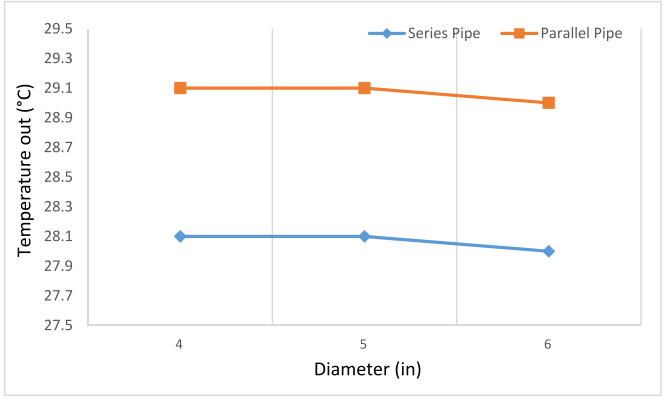

Fig. 7. Effect of EAHE pipe diameter on the outlet air temperature.

5.3. The effect of ground surface covers on the outlet air temperature of EAHE

The types of ground surface covers may affect the solar energy absorption into the soil domain. The performance of the EAHE is examined in this research across various ground surface covers with different albedo values impacting surface temperature (Refer to Table 8). **Equation (4)** is used to calculate the temperature for various ground surface covers.

Based on the simulation results, Fig. 8 depicts the effect of ground surface covers on the outlet air of EAHE for a cooling application. It can be observed that the EAHE yields the lowest air temperature when operating under a short grass soil cover, with a value of 27.8 °C and 29 °C for series and parallel arrangements, respectively. On the contrary, the EAHE with an asphalt surface cover produces the highest outlet air temperature among others, namely 28.7 °C for series arrangement and 29.5 °C for parallel arrangement. The presence of asphalt on the ground surface can hinder the transfer of heat as a result of its poor thermal conductivity and heat absorption properties. Meanwhile, the performance of EAHE with bare soil or concrete cover is in the range between short grass soil and asphalt cover. The EAHE with bare soil surface attains a relatively lower outlet air temperature namely 28.1 °C and 29.2 °C for series and parallel arrangements, respectively. The findings show that the soil surface covers affect the performance of EAHE. Soil surface coverings can change the circumstances of heat transfer between the ground and the air as it moves through the EAHE system.

The reflective properties of soil surface covers, also known as albedo, play a crucial role in influencing the efficiency of earth air heat exchangers (EAHEs). The short grass soil surface has an albedo value of 0.16 and a thermal diffusivity of 3.29×10^{-7} m^2/s, which is the lowest when compared to other types of surfaces, followed by soil, concrete, and asphalt. The variation in albedo value impacts the quantity of solar energy assimilated by the encompassing ground of the EAHE system. Higher albedo surfaces can reflect a greater amount of sunlight, which in turn decreases the heat absorbed by the ground. This subsequently results in the reduction of the temperature of the soil surrounding the EAHE system. Consequently, the air that passes through the EAHE system will encounter cooler temperatures, thereby improving the efficiency of the cooling process. On the contrary, lower albedo surfaces tend to absorb more solar radiation, leading to higher ground temperatures [45]. This can potentially diminish the effectiveness of the EAHE system, especially in cooling applications. Therefore, the selection of soil surface covers with higher albedo values can enhance the performance of EAHE systems by optimising the thermal conditions of the surrounding soil and improving heat exchange processes.

5.4. Pressure drop

The correlation between EAHE's pipe length and pressure drop is shown in Fig. 9 for both series and parallel arrangements, considering a pipe diameter of 4 in. The graphic illustrates that the pressure drop increases in direct proportion to the lengthening of the EAHE pipe. Generally, the friction loss is increased by pipe length due to a greater surface area for interaction with fluid. In the series system, the fluid passes sequentially through each heat exchanger, thus, the pressure drop in each exchanger accumulates along the flow route. This cumulative effect causes the heat exchanger to experience a greater pressure loss.

Table 8
Ground surface cover temperature.

Material	Albedo	Surface Temperature °C
Bare Soil	0.3	32.11
Short Grass Soil	0.16	32.07
Asphalt	0.1	32.05
Concrete	0.25	32.09

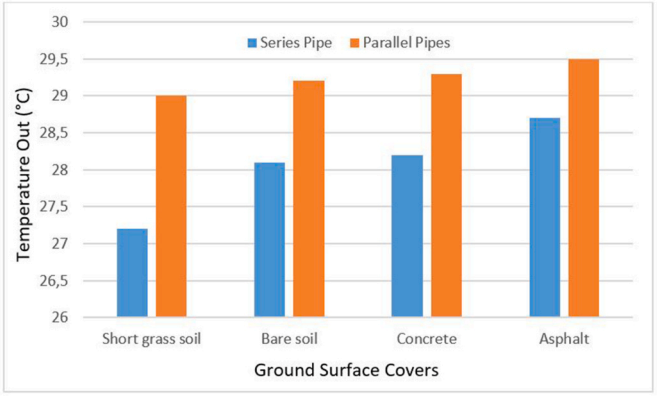

Fig. 8. Effect of ground surface type on the EAHE's outlet air temperature.

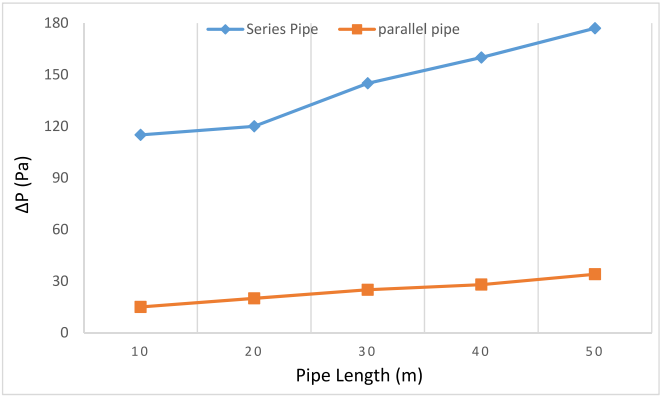

Fig. 9. Effect of pipe length on pressure drop.

While, in parallel arrangements, the fluid is separated and flows through several heat exchangers at the same time before being re-united. The distribution of airflow among the parallel pipes is uneven and influenced by various geometric factors, most notably the relationship between parallel pipes and manifold diameters, as well as the length of branch pipes [46]. The aerodynamic imbalance in the airflow happens within each parallel EAHE pipe branch due to the manifolds and branch pipes having the same diameter, and also when a short pipe (with a length less than a hundred times its diameter) is present. This condition leads to a notable decrease in thermal efficiency [47]. EAHE with a manifolds' diameter larger than the branch pipes experience significantly improved air distribution uniformity due to the presence of much higher pressure losses in the parallel branch pipes compared to the manifolds [47]. The parallel EAHE owns a smaller overall pressure loss as compared to series configurations. This is because the flow path per heat exchanger can be shorter, resulting in fewer frictional losses. This analysis validates the reason for the significantly high-pressure drop in the series arrangement. As can be seen from the figure, the EAHE with a total length of 50 m generates 177 Pa and 34 Pa of pressure drop for series and parallel arrangements, respectively. Thus, understanding this relationship is critical in designing piping systems with adequate operating needs while conserving energy and maintaining proper fluid pressure throughout the system. The modelling results indicate that the pressure drop in the series configuration is approximately six times higher than in the parallel arrangement. Single-pipe exchangers have the potential to replace multi-pipe exchangers in thermal efficiency, but they result in increased pressure losses, leading to higher energy consumption for the fan drive. A study conducted by Amanowicz and Wojtkowiak [48] reveals that the replacement of multi-pipe EAHEs is possible with single-pipe structures of a larger diameter while maintaining comparable energy performance and electricity consumption.

5.5. Soil temperature contour adjacent to EAHE

The temperature of the surrounding soil has a significant impact on the performance of an EAHE. It's crucial to have a comprehensive grasp of the soil temperature profile to achieve the best design and operation of the EAHE system. This system utilises the constant temperature of the earth to condition incoming air. Generally, the profile of soil temperature is influenced by two heat sources. In the upper part, the soil temperature gradient is mostly affected by the heat mechanism occurring on the ground surface. In general, it is common for soil temperatures to experience fluctuations in response to seasonal shifts when observed closer to the surface. However, as one delves deeper into the soil, these fluctuations tend to decrease in intensity and ultimately reach a state of stability in terms of temperature. The soil temperature surrounding the EAHE displays a gradient, characterised by elevated temperatures closer to the surface of the EAHE, and diminishes as the distance to the surface increases. This phenomenon is due to the heat dissipation of EAHE.

Figs. 10 and **11** illustrate the air and soil temperature profiles, for the series and parallel arrangements, respectively. Fig. 10 shows that heat penetration from the pipe surface to the soil is highest upstream of the EAHE (0–12 m) due to the large temperature difference between the inlet air and the surrounding soil and decreases as the pipe distance increases as the air is cooled along the EAHE. For the parallel arrangement (see Fig. 11), it can be observed that the heat penetration into the soil domain is almost evenly distributed. This tendency is due to the air from the inlet manifold being split into several pipes (that have the same length), which then releases approximately the same amount of heat to the surrounding soil.

5.6. Effectiveness-NTU of EAHE

Fig. 12 illustrates the relationship between effectiveness and NTU of the EAHE obtained based on three different EAHE pipe diameters, namely, 4 in, 5 in, and 6 in. It was found that the effectiveness of parallel and series arrangements of EAHE is proportional to NTU. The same trend in the effectiveness-NTU result is also presented by Yusof et al. [1]. The NTU value is affected by EAHE pipe diameter. The larger the EAHE diameter, the higher the NTU value, as the diameter affects the velocity of the air inside the EAHE and results in lower outlet air temperature. The effectiveness value for parallel and series EAHE arrangements increases with increasing NTU value. This relationship is obtained based on the calculated results of **Equation (10)**. In addition, it is demonstrated that the parallel EAHE has an average 15 % higher value in effectiveness than a series arrangement. The heat transfer process tends to be more efficient in parallel arrangements due to improved utilisation of surface area and decreased thermal gradients, resulting in higher efficiency.

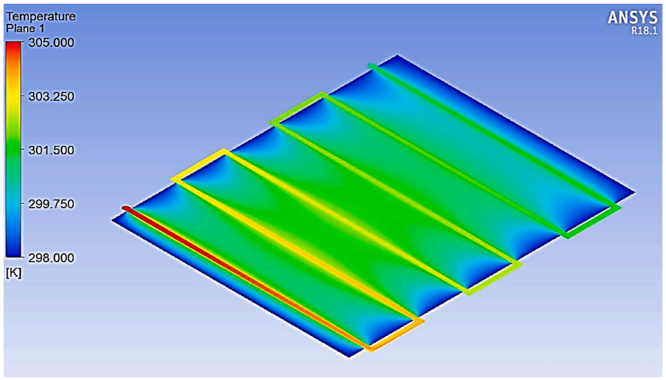

Fig. 10. Soil temperature contour adjacent to the series arrangement of EAHE.

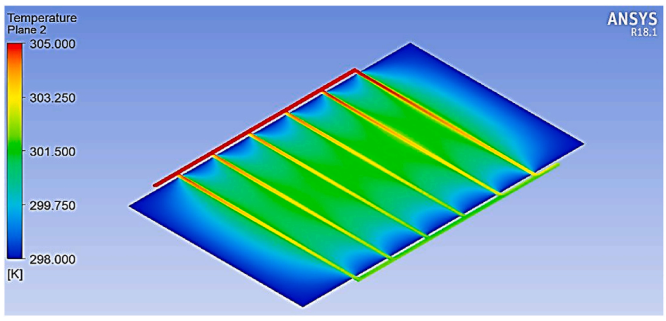

Fig. 11. Soil temperature contour adjacent to the parallel arrangement of EAHE.

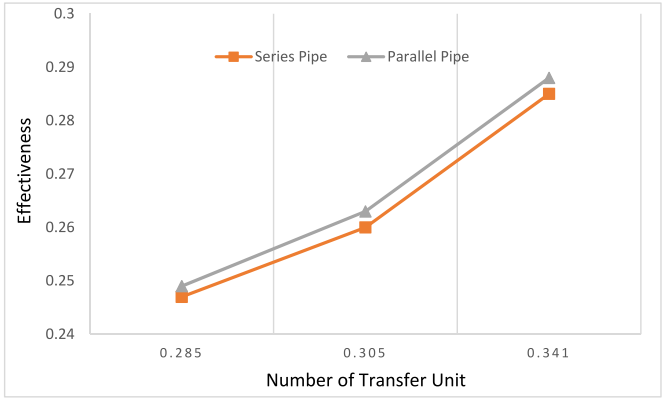

Fig. 12. The relationship effectiveness-NTU.

6. Conclusion

The thermal performance comparison between series and parallel configurations of EAHE is illustrated in this research through CFD simulation. The findings of this study are summarised as follows.

1. In terms of thermal performance, it was demonstrated that the series arrangement heat exchanger can achieve a lower outlet temperature compared to the parallel arrangement. Due to its longer airflow path, this design enables the maximisation of heat transfer efficiency by gradually pre-cooling the air. In contrast, parallel arrangements operate independently and do not benefit from this cumulative cooling effect.
2. Based on variations in pipe length for both series and parallel arrangements of EAHE, the simulation results reveal that the decrease in EAHE outlet air temperature is directly proportional to increasing pipe length. This is owing to the fact that a longer EAHE provides a bigger surface area for heat exchange with the surrounding soil, hence increasing the heat transfer capabilities.
3. The variations of EAHE's pipe diameter show that the decrease in outlet air temperature is directly proportional to the increase in the diameter of the heat exchanger, although it does not decrease significantly. Increasing the EAHE diameter not only causes an increase in the heat transfer area but also slows airflow inside EAHE, so it affects the heat transfer rate of EAHE.
4. The effect of ground surface covers shows that the short grass surface provides the best EAHE performance, thus it is a very suitable surface cover for EAHE. The grassy soil has an albedo value of 0.16 and is able to reduce the exit air temperature to 27.8 °C.
5. Based on the simulation results, it was found that variations in pipe length affect the EAHE pressure drop. This is because frictional losses rise with pipe length as the fluid interacts with a larger surface area.

It was found that when considering pressure drop, parallel pipe geometries outperform the series pipe geometries.

6. The results of the effectiveness-NTU relationship show that effectiveness is directly proportional to NTU. Research has shown that the parallel EAHE exhibits, on average, a 15 % greater effectiveness compared to a series configuration. This is attributed to the improved utilisation of surface area and minimised thermal gradients, resulting in enhanced efficiency during the heat transfer process.

CRediT authorship contribution statement

Sarwo Edhy Sofyan: Writing – original draft, Resources, Methodology, Investigation, Formal analysis. **Teuku Meurah Indra Riayatsyah:** Writing – review & editing, Visualization, Validation. **Khairil:** Writing – review & editing, Validation. **Eric Hu:** Visualization, Validation, Conceptualization. **Akram Tamlicha:** Writing – review & editing, Validation. **Teuku Muhammad Reza Pahlefi:** Investigation, Formal analysis. **H.B. Aditiya:** Writing – review & editing, Validation.

Declaration of competing interest

The authors declare that they have no known competing financial interests or personal relationships that could have appeared to influence the work reported in this paper.

Data availability

Data will be made available on request.

Acknowledgement

The authors wish to acknowledge with many thanks to Universitas Syiah Kuala, Minister of National Education of the Republic of Indonesia for financing the research through the H-Index Grant Program: Publication scheme 2022 No.:144/UN11/SPK/PNBP/2022.

Nomenclature

$T_{soil\ (Z,t)}$	Soil temperature at depth Z of the soil surface and at time t of year, °C
T_{mean}	Average ground surface temperature (or average annual air temperature), °C
T_{amp}	Ground surface temperature amplitude, °C
Z	Depth from ground level, m
α	Soil thermal diffusivity, mm^2/day
t_{year}	current time, day
t_{shift}	Day of the year for lowest ground surface temperature, day
$d = \sqrt{\frac{2\alpha}{\omega}}$	Constant phase
Q	Heat Flux at ground level, W/m^2
R_{sol}	Total solar radiation, W/m^2
R_{sky}	Wavelength of radiation to earth, W/m^2
R_{surf}	Wavelength of solar radiation from the earth's surface, W/m^2
H_{surf}	Heat Flux sensible, W/m^2
L_{surf}	Heat Flux latent, W/m^2
SAT	Soil air temperature, °C
θ_0	Ambient temperature, °C
α_0	Overall heat transfer coefficient between soil and air, $W/(m^2K)$
α_S	Albedo
J	Total solar radiation, W/m^2
ε	wavelength emissivity, 0.9
J_{eh}	effective emission, W/m^2
Q_{total}	heat received or released, J
m_{air}	mass flow rate, kg/s
$C_{p,air}$	specific heat value of air, J/(kgK)
T_{air}	Air temperature, °C
h	Convection coefficient, $W/(m^2K)$
A	Heat transfer area, m^2
T_{wall}	soil temperature, °C
$T_{air,out}$	pipe outlet air temperature, °C
$T_{air,in}$	pipe inlet air temperature, °C
q'_{sp}	Flux entering the pipe at the surface, W/m
h_{sp}	Convection coefficient, $W/(m^2K)$
D	Pipe diameter, m
T_{sp}	Pipe surface inlet temperature, K
T_{ap}	Air inlet temperature, K
q'_{sse}	Flux entering the soil surface, W/m^2
$q''_{con\ v}$	Convection flux, W/m^2
q''_{swr}	Radiation shortwave flux, W/m^2
q''_{lwr}	Radiation longwave flux, W/m^2
L_{infl}	Earth-air heat exchanger length, m
Q	Total hourly cooling of the system, J/hr

$\dot{m}$	Mass flow rate of air in the pipe, kg/s
C	discharge coefficient/release
c	Specific heat of air, J/kgK
T	Air inlet temperature, K
T_{out}	Air exit temperature, K

References

[1] T.M. Yusof, H. Ibrahim, W.H. Azmi, M.R.M. Rejab, Thermal analysis of earth-to-air heat exchanger using laboratory simulator, Appl. Therm. Eng. 134 (July 2017) (2018) 130–140, https://doi.org/10.1016/j.applthermaleng.2018.01.124.

[2] H. Sadighi Dizaji, E.J. Hu, L. Chen, A comprehensive review of the Maisotsenko-cycle based air conditioning systems, Energy 156 (2018) 725–749, https://doi.org/10.1016/j.energy.2018.05.086.

[3] Z. Zhang, J. Sun, Z. Zhang, X. Jia, Y. Liu, Numerical research and parametric study on the thermal performance of a vertical earth-to-air heat exchanger system, Math. Probl Eng. 2021 (2021), https://doi.org/10.1155/2021/5557280.

[4] N. Rosa, N. Soares, J.J. Costa, P. Santos, H. Gervásio, Assessment of an earth-air heat exchanger (EAHE) system for residential buildings in warm-summer Mediterranean climate, Sustain. Energy Technol. Assessments 38 (2020) 100649, https://doi.org/10.1016/j.seta.2020.100649.

[5] J. Xiao, Q. Wang, X. Wang, Y. Hu, Y. Cao, J. Li, An earth-air heat exchanger integrated with a greenhouse in cold-winter and hot-summer regions of northern China: modeling and experimental analysis, Appl. Therm. Eng. 232 (2023) 120939, https://doi.org/10.1016/j.applthermaleng.2023.120939.

[6] J. Xiao, J. Li, Influence of different types of pipes on the heat exchange performance of an earth-air heat exchanger, Case Stud. Therm. Eng. 55 (2024) 104116, https://doi.org/10.1016/j.csite.2024.104116.

[7] V.M. Maytorena, J.F. Hinojosa, S. Moreno, D.A. Buentello-Montoya, Thermal performance analysis of a passive hybrid earth-to-air heat exchanger for cooling rooms at Mexican desert climate, Case Stud. Therm. Eng. 41 (November 2022) (2023) 102590, https://doi.org/10.1016/j.csite.2022.102590.

[8] S.E. Sofyan, K. Khairil, Z. Maulana, A. Tamlicha, Jalaluddin, M. Syaukani, Development of CFD simulation model of earth air heat exchanger for space cooling of a 36 M2 house in tropical climate Banda Aceh, Indonesia, Polimesin 21 (2) (2023) 170–178 [Online]. Available: http://e-jurnal.pnl.ac.id/polimesin/article/view/3692.

[9] M. Rana, M.M. Nuhash, A.A. Bhuiyan, A CFD modelling for optimizing geometry parameters for improved performance using clean energy geothermal ground-to-air tunnel heat exchangers, Case Stud. Therm. Eng. 53 (November 2023) (2024) 103867, https://doi.org/10.1016/j.csite.2023.103867.

[10] S.F. Ahmed, M.M.K. Khan, M.T.O. Amanullah, M.G. Rasul, N.M.S. Hassan, A parametric analysis of the cooling performance of vertical earth-air heat exchanger in a subtropical climate, Renew. Energy 172 (2021) 350–367, https://doi.org/10.1016/j.renene.2021.02.086.

[11] Y. Zhao, R. Li, C. Ji, C. Huan, B. Zhang, L. liu, Parametric study and design of an earth-air heat exchanger using model experiment for memorial heating and cooling, Appl. Therm. Eng. 148 (2019) 838–845, https://doi.org/10.1016/j.applthermaleng.2018.11.018.

[12] A. Aranda-Arizmendi, M. Rodríguez-Vázquez, C.M. Jiménez-Xamán, R.J. Romero, M. Montiel-González, Parametric study of the ground-air heat exchanger (GAHE): effect of burial depth and insulation length, Fluid 8 (2) (2023), https://doi.org/10.3390/fluids8020040.

[13] M.I. Hasan, S.W. Noori, A.J. Shkarah, Parametric study on the performance of the earth-to-air heat exchanger for cooling and heating applications, Heat Tran. Res. 48 (5) (Jul. 2019) 1805–1829, https://doi.org/10.1002/htj.21458.

[14] A.A. Hegazi, O. Abdelrehim, A. Khater, Parametric optimization of earth-air heat exchangers (EAHEs) for central air conditioning, Int. J. Refrig. 129 (2021) 278–289, https://doi.org/10.1016/j.ijrefrig.2021.05.009.

[15] Q. Li, H. Su, Y. Lyu, S. Wei, Annual thermal performance analysis and optimization of earth-air heat exchanger by using a new 1D-2D hybrid numerical model, J. Build. Eng. 71 (2023) 106526, https://doi.org/10.1016/j.jobe.2023.106526.

[16] Ł. Amanowicz, J. Wojtkowiak, Validation of CFD model for simulation of multi-pipe earth-to-air heat exchangers (EAHEs) flow performance, Therm. Sci. Eng. Prog. 5 (October 2017) (2018) 44–49, https://doi.org/10.1016/j.tsep.2017.10.018.

[17] Ł. Amanowicz, Influence of geometrical parameters on the flow characteristics of multi-pipe earth-to-air heat exchangers – experimental and CFD investigations, Appl. Energy 226 (March) (2018) 849–861, https://doi.org/10.1016/j.apenergy.2018.05.096.

[18] A. Minaei, R. Rabani, Development of a transient analytical method for multi-pipe earth-to-air heat exchangers with parallel configuration, J. Build. Eng. 73 (2023) 106781, https://doi.org/10.1016/j.jobe.2023.106781.

[19] C.-Y. Hsu, P.-C. Huang, J.-D. Liang, Y.-C. Chiang, S.-L. Chen, The in-situ experiment of earth-air heat exchanger for a cafeteria building in subtropical monsoon climate, Renew. Energy 157 (2020) 741–753, https://doi.org/10.1016/j.renene.2020.05.009.

[20] D. Qi, S. Li, C. Zhao, W. Xie, A. Li, Structural optimization of multi-pipe earth to air heat exchanger in greenhouse, Geothermics 98 (2022) 102288, https://doi.org/10.1016/j.geothermics.2021.102288.

[21] D. Qi, Q. Liu, C. Zhao, S. Li, B. Song, A. Li, Optimizing the thermal environment of greenhouse with multi-pipe earth-to-air heat exchanger system using the Taguchi method, Appl. Therm. Eng. (2024) 122469, https://doi.org/10.1016/j.applthermaleng.2024.122469.

[22] K.K. Agrawal, M. Bhardwaj, R. Misra, G. Das Agrawal, V. Bansal, Optimization of operating parameters of earth air tunnel heat exchanger for space cooling: taguchi method approach, Geoth. Energy 6 (1) (2018) 1–17, https://doi.org/10.1186/s40517-018-0097-0.

[23] Y. Lin, et al., A study on the optimal air, load and source side temperature combination for a variable air and water volume ground source heat pump system, Appl. Therm. Eng. 178 (June) (2020) 115595, https://doi.org/10.1016/j.applthermaleng.2020.115595.

[24] S.E. Sofyan, E. Hu, A. Kotousov, Modelling of a horizontal geo heat exchanger with an internal source term approach, Energy Proc. 61 (2014) 104–108, https://doi.org/10.1016/j.egypro.2014.11.917.

[25] S.E. Sofyan, E. Hu, A. Kotousov, T.M.I. Riayatsyah, R. Thaib, Mathematical modelling and operational analysis of combined vertical⇓horizontal heat exchanger for shallow geothermal energy application in cooling mode, Energies 13 (24) (2020), https://doi.org/10.3390/en13246598.

[26] A. Delazar, E. Hu, A. Kotousov, Geothermics A novel three-dimensional implicit numerical model of a borehole field heat exchanger that accounts for seasonal fluctuations of the soil temperature, Geothermics 97 (July) (2021) 102236, https://doi.org/10.1016/j.geothermics.2021.102236.

[27] T. Kusuda, P. Achenbach, Earth temperatures and thermal diffusivity at selected stations in the United States, Build. Eng. 71 (1) (1965) 61–74 [Online]. Available: http://care.diabetesjournals.org/content/34/Supplement_1/S89.full.pdf.

[28] H. Ben Jmaa Derbel, O. Kanoun, Investigation of the ground thermal potential in Tunisia focused towards heating and cooling applications, Appl. Therm. Eng. 30 (10) (2010) 1091–1100, https://doi.org/10.1016/j.applthermaleng.2010.01.022.

[29] C.O. Popiel, J. Wojtkowiak, B. Biernacka, Measurements of temperature distribution in ground, Exp. Therm. Fluid Sci. 25 (5) (2001) 301–309, https://doi.org/10.1016/S0894-1777(01)00078-4.

[30] H. Li, W. Xu, Z. Yu, J. Wu, Z. Sun, Application analyze of a ground source heat pump system in a nearly zero energy building in China, Energy 125 (2017) 140–151, https://doi.org/10.1016/j.energy.2017.02.108.

[31] A.N.Z. Sanusi, L. Shao, N. Ibrahim, Passive ground cooling system for low energy buildings in Malaysia (hot and humid climates), Renew. Energy 49 (2013) 193–196, https://doi.org/10.1016/j.renene.2012.01.033.

[32] H. Wu, S. Wang, D. Zhu, Modelling and evaluation of cooling capacity of earth–air–pipe systems, Energy Convers. Manag. 48 (5) (2007) 1462–1471, https://doi.org/10.1016/j.enconman.2006.12.021.

[33] M.C. Lekhal, M.-H. Benzaama, A. Kindinis, A.-M. Mokhtari, R. Belarbi, Effect of geo-climatic conditions and pipe material on heating performance of earth-air heat exchangers, Renew. Energy 163 (2021) 22–40, https://doi.org/10.1016/j.renene.2020.08.044.

[34] H. Yilmaz, S. Toy, M.A. Irmak, S. Yilmaz, Y. Bulut, Determination of temperature differences between asphalt concrete, soil and grass surfaces of the City of Erzurum, Turkey, Atmósfera 21 (2) (2008) 135–146.

[35] H. Fujii, S. Yamasaki, T. Maehara, T. Ishikami, N. Chou, Numerical simulation and sensitivity study of double-layer Slinky-coil horizontal ground heat exchangers, Geothermics 47 (2013) 61–68, https://doi.org/10.1016/j.geothermics.2013.02.006.

[36] T.L. Bergman, A. Lavine, F. Incropera, Fundamentals of Heat and Mass Transfer, John Wiley & Sons, Ltd, 2011. Seventh., no. september 2016.

[37] T.S. Bisoniya, A. Kumar, P. Baredar, Study on calculation models of earth-air heat exchanger systems, J. Energy 2014 (2014) 1–15, https://doi.org/10.1155/2014/859286.

[38] T. Manik, Tulus Burhanuddin Sitorusa, Andi Syahputra, Performance of earth air heat exchanger using closed cycle in Medan city, J. Sist. Tek. Ind. 22 (1) (2020) 63–76, https://doi.org/10.32734/jsti.v22i1.3274.

[39] L. Ramírez-Dávila, J. Xamán, J. Arce, G. Álvarez, I. Hernández-Pérez, Numerical study of earth-to-air heat exchanger for three different climates, Energy Build. 76 (2014) 238–248, https://doi.org/10.1016/j.enbuild.2014.02.073.

[40] J.M. Rivero, F. Méndez Lavielle, Earth-air thermal siphon as a passive air-conditioning system for an arid climate, Int. J. Heat Mass Tran. 210 (2023) 124171, https://doi.org/10.1016/j.ijheatmasstransfer.2023.124171.

[41] D. Zhang, J. Zhang, C. Liu, C. Yan, J. Ji, Z. An, Performance measurement and configuration optimization based on orthogonal simulation method of earth-to-air heat exchange system in cold-arid climate, Energy Build. 308 (2024) 114001, https://doi.org/10.1016/j.enbuild.2024.114001.

[42] S. Thiers, B. Peuportier, Thermal and environmental assessment of a passive building equipped with an earth-to-air heat exchanger in France, Sol. Energy 82 (9) (2008) 820–831, https://doi.org/10.1016/j.solener.2008.02.014.

[43] A.A. Hegazi, O. Abdelrehim, A. Khater, Parametric optimization of earth-air heat exchangers (EAHEs) for central air conditioning, Int. J. Refrig. 129 (2021) 278–289, https://doi.org/10.1016/j.ijrefrig.2021.05.009.

[44] Maoz, et al., Parametric optimization of earth to air heat exchanger using response surface method, Sustainability 11 (11) (2019), https://doi.org/10.3390/su11113186.

[45] A. Farahat, H.D. Kambezidis, S.I. Kampezidou, Effect of the ground albedo on the estimation of solar radiation on tilted flat-plate surfaces: the case of Saudi arabia, Energies 16 (23) (2023), https://doi.org/10.3390/en16237886.
[46] Ł. Amanowicz, J. Wojtkowiak, Approximated flow characteristics of multi-pipe earth-to-air heat exchangers for thermal analysis under variable airflow conditions, Renew. Energy 158 (2020) 585–597, https://doi.org/10.1016/j.renene.2020.05.125.
[47] Ł. Amanowicz, J. Wojtkowiak, Thermal performance of multi-pipe earth-to-air heat exchangers considering the non-uniform distribution of air between parallel pipes, Geothermics 88 (May) (2020) 101896, https://doi.org/10.1016/j.geothermics.2020.101896.
[48] Ł. Amanowicz, J. Wojtkowiak, Comparison of single- and multipipe earth-to-air heat exchangers in terms of energy gains and electricity consumption: a case study for the temperate climate of central europe, Energies 14 (24) (2021), https://doi.org/10.3390/en14248217.